JOURNAL OF AGRICULTURAL AND FOOD CHEMISTRY

J. Agric. Food Chem. **2002,** *50,* 3179−3185 **3179**

Structural Changes in Apple Rings during Convection Air-Drying with Controlled Temperature and Humidity

YAN BAI,[†] M. SHAFIUR RAHMAN,*[,†] CONRAD O. PERERA,[†,‡] BRONWEN SMITH,[§] AND LAURENCE D. MELTON[§]

Horticulture and Food Research Institute of New Zealand, Private Bag 92 169, Auckland, New Zealand, and Food Science Postgraduate Programme, The University of Auckland, Private Bag 92 019, Auckland, New Zealand

The structure of heat pump dried apple slices, developed as a function of air temperature and constant humidity, was studied by measuring porosity and using electron microscopy. The porosity of the apple rings increased linearly when the moisture content decreased during drying and then reached a constant value. In all dried apple slices, a degree of cellular collapse occurred. Case hardening occurred in the surface of the dried tissue when the apple slices were dried at 40−45 and 60−65 °C, and in the extreme case (at 60−65 °C) cracks were formed on the surface.

KEYWORDS: Apple; heat pump drying; structure; convection drying; electron microscopy

INTRODUCTION

Drying in earlier times was done in the sun. Now many types of sophisticated equipment and methods are being used to dehydrate foods. Recently, heat pump drying of foods and bioactive materials has gained high interest from industry. The heat pump works in the same way as a refrigerator, with an evaporator, which absorbs heat, and a condenser, which emits heat, effectively pumping heat from a low-temperature evaporator to a high-temperature condenser. The dry heated air is supplied continuously to the product to pick up moisture. The humid air passes through the evaporator of the heat pump where it condenses, thus giving up its latent heat of vaporization to the refrigerant in the evaporator. This heat is used to reheat the cool dry air passing over the hot condenser of the heat pump. Thus, in a heat pump the latent heat recovered in the process is released at the condenser of the refrigeration circuit and used to reheat the air within the dryer (*1*, *2*). The heat pump drier differs from conventional air-drying in that very controlled humidity and temperature are maintained and a completely closed system is provided. In conventional air-drying, the air humidity increases with the progress of drying by continuous air saturation due to loss of moisture from the product. Thus, humidity could not be controlled. In heat pump drying (HPD) adequate control of humidity and temperature can be maintained. Heat pump dryers offer several advantages over conventional hot-air driers for the drying of food products. These include higher energy efficiency, better product quality, the ability to operate independently of outside ambient weather conditions, and positive environmental impact due to low energy requirement and no release of volatile components to the environment (*2*). Although a number of studies have been published on the drying kinetics (*3*), microbiological changes (*4*), development of brown center (*5*, *6*), and volatile retention (*1*) of food products during HPD, structural changes associated with HPD have not been studied.

Foods have a structure imparted by nature, which can be modified by processing. The structure of food is an important quality parameter for dried products. Modern microscopy techniques assist in visualization of the structures (*7*−*9*). Other methods used for studying pore characteristics are mercury porosimetry, gas adsorption method, and helium gas pycnometry (*10*). Rahman (*11*) compiled data on pore formation in a few foods during drying. Application of microscopy techniques for studying the microstructure of a variety of foods and food model systems was presented by Gejl-Hansen and Flink (*12*). They applied microscopy techniques to the description of structure of freeze-dried food systems. They also identified the spatial distribution of components of complex multiphase systems, which was useful for understanding the physical and chemical properties of the complex material. The microscopy studies indicated that organic compounds of limited aqueous solubility retained in the freeze-dried product were in the form of liquid droplets. These droplets develop during cooling and freezing and are entrapped in the interstitial matrix after freezing (*13*). Furthermore, droplets of volatile compounds are locked into the dry material following the freeze-drying step. The microstructure of some selected freeze-dried oil-in-water emulsions was also investigated by microscopy (*14*). In that study the separation of the lipid phase into surface and encapsulated fractions was quantitatively evaluated. However, there is little information on the structural characteristics of products dried

* Address correspondence to this author at the Department of Bioresource and Agricultural Engineering and Department of Food Science and Nutrition, College of Agriculture, Sultan Qaboos University, P.O. Box 34, Al Khod 123, Muscat, Sultanate of Oman (e-mail shafiur@squ.edu.om).

[†] Horticulture and Food Research Institute of New Zealand.

[‡] Present address: Department of Chemistry, The National University of Singapore, 3 Science Drive, Singapore 117543.

[§] The University of Auckland.

10.1021/jf011354s CCC: $22.00
Published on Web 04/27/2002

with a heat pump, which permits the precise control of both air humidity and temperature.

The structure of dried materials depends on the drying methods and conditions. In heat pump drying, diversified structural characteristics of the dried material could be generated using a wide range of operating conditions, which are not possible in conventional air-drying. For example, conventional air-drying could not be performed at 20 °C due to high air humidity. However, the drying can be performed even at 0 °C by reducing the air humidity to a very low level in the case of heat pump drying; thus, varied structural characteristics could be developed using different combinations of temperature and humidity. The objective of this work was to study the structure of heat pump (controlled temperature and humidity) dried apple slices by measuring porosity and using electron microscopy.

MATERIALS AND METHODS

Sample Preparation. Pacific Rose apples (*Malus domestica* Borkh. cv. Pacific Rose) were purchased from a local supermarket in Auckland, New Zealand, and stored at 0−5 °C for 7−10 days until used. The apples were removed from the cool room and then cut into cylinders using a hollow steel cylinder of 60 mm diameter with a sharp edge. The apple cylinders were then cut into 10 mm slices, and cores were removed using a hollow steel cylinder of 25 mm diameter with a sharp edge to form annular rings. Only the middle three to four annular rings per apple were taken for the experiment. Particle density, apparent density, and substance density of the dried apples at different moisture contents were measured by a helium gas pycnometer. The moisture content was measured gravimetrically by drying tissue in a vacuum oven at 70 °C for at least 18 h.

Heat Pump Drying. A pilot scale heat pump dryer located at HortResearch was used to study apple drying. Specifications of the drier are given by Rahman et al. (*3*). Apple slices were placed in a single layer on a wire mesh tray (38 × 27 cm). Air flow was maintained parallel to the two major surfaces of the layer, permitting drying from both surfaces. The drying temperature was varied from 20 to 65 °C, and the air velocity was maintained constant at 1.5 m/s. The dryer was turned on to reach the desired temperature and humidity level (20−25%). The tray containing apple slices was then placed on an built-in weighing balance inside the drying chamber. Apple slices were removed from the heat pump drier following 24 h of drying and examined by scanning electron microscopy.

Density Measurement. The geometric dimensions of the fresh and dried samples were measured using a slide caliper, and apparent volume was calculated using a gas pycnometer on the samples coated with wax. Apparent density and substance density of the dried apples as a function of moisture contents were measured using a helium gas pycnometer (VM-100, Ku and Kyoto, Japan). To measure the apparent density, apple rings were cut in half, so that the halves would fit into the sample holder. Samples were then weighed before and after coating (six coats in total) with paraffin wax (setting range ∼55−60 °C). The substance density of dried powder was measured as follows: the dried apple slices (zero moisture content) were ground into a fine powder. The powder was then placed in the sample holder of the helium gas pycnometer. The substance density was calculated using the mass of the sample divided by the volume of the sample measured by the gas pycnometer. The substance density of the sample at other moisture contents was estimated using the equation (*11*)

$$\frac{1}{\rho_s} = \frac{X_w}{\rho_w} + \frac{X_s}{\rho_s^0} \quad (1)$$

where ρ_s is the substance density in different moisture contents (kg/m^3), ρ_s^0 is the substance density of ground dried apple powder at zero moisture content (kg/m^3), ρ_w density of water (kg/m^3), x_w mass fraction of water (wet basis), and x_s is the mass fraction of solids (wet basis). The main assumption in the above equation is that the material having multicomponents follows the conservation of mass and volume; that is, the excess volume due to the components' interaction is negligible. The apparent porosity is the volume ratio of all the pores and the volume of the material, which was calculated as (*11*)

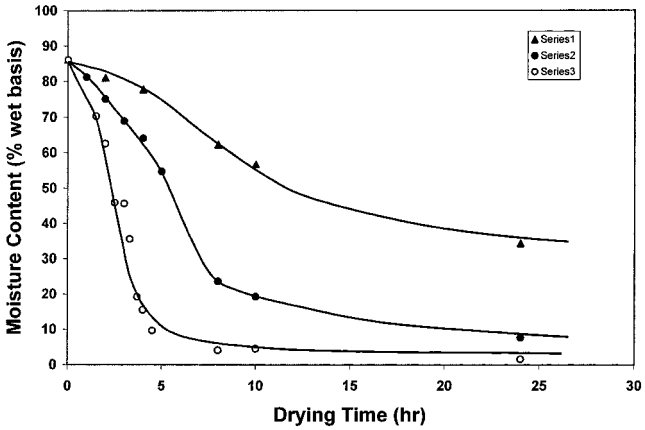

Figure 1. Moisture content of dried apple as a function of drying time: series 1, drying temperature = 20–25 °C; series 2, drying temperature = 40–45 °C; series 3, drying temperature = 60–65 °C).

$$\epsilon_a = 1 - (\rho_a/\rho_s) \quad (2)$$

where ϵ_a is the apparent porosity and ρ_s and ρ_a are the substance and apparent densities (kg/m^3), respectively. The apparent shrinkage during processing can be defined as the ratio of the apparent volume at any moisture content and initial apparent volume of the materials before processing. Apparent shrinkage was calculated from the equation

$$S_a = (V_a/V_a^0) \quad (3)$$

where S_a, V_a, and V_a^0 are the apparent shrinkage, volume of the sample at any moisture content, and volume of sample before drying (m^3), respectively.

Scanning Electron Microscopy. Fresh apple cubes (10 mm× 5 mm× 5 mm) were placed successively in 5 mL bottles containing solutions of ethanol of increasing concentration (30, 50, 70, and 100%) for 5 min each. The cubes were then transferred into another 5 mL bottle containing 100% ethanol. The apple cubes were then placed into the critical point drier (CPD) for 90 min, after which time the ethanol had evaporated and the dried apple samples were removed. The apple cubes (dried by CPD and HPD) were then cut into sections (2−4 mm thick) so that the interior and exterior surfaces could be imaged. A 1:1 mixture of Araldite (super strength) epoxy resin and epoxy hardener was used to adhere the sections to 10 mm diameter stubs. Sections were sputter coated with gold to a thickness of 50 nm. Samples of fresh apple (dried by CPD) and dried apple (dried by HPD) were coated with gold on a cooling stage to a thickness of 50 nm. Images were obtained using a scanning electron microscope (XL 30s FEG PHILIPS, Eindhoven, The Netherlands) at an accelerating voltage of 500 kV.

RESULTS AND DISCUSSION

Drying Curve. The drying curves of heat pump dried apple slices are shown in **Figure 1**. **Figure 1** shows that there was no lag period and that the moisture content of the apple decreased with the increase in drying time. The moisture content of the apple slices dried at 20−25 °C decreased slowly from 86 to 34% (wet basis) after 24 h of drying. In comparison, the apple slices dried at 40−45 °C showed a faster moisture loss. Furthermore, moisture loss was faster in the first 10 h, during which time the moisture content dropped to 19.21%. Thereafter, the rate slowed until the moisture content was 7.67%, after 24 h. Apple slices at 60−65 °C showed fastest moisture loss. The greatest loss occurred in the first 10 h, during which time the moisture content dropped to 4.05%. The moisture content was close to zero (2.0%) after 24 h. The drying curves provide the

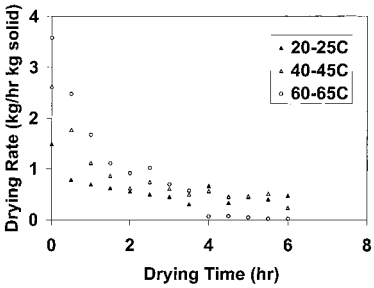

Figure 2. Drying curves of apple samples at different temperatures.

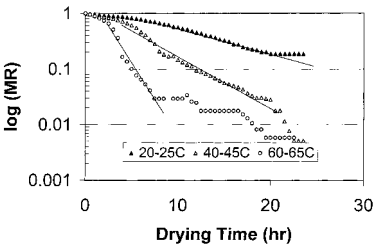

Figure 3. Plot of log(MR) with drying time as a function of drying temperatures.

time required to dry apple slices to predetermined moisture content at these temperatures. Thus, if the moisture content of dried apple has to be reduced 60%, the drying time would be ~10 h at 20−25 °C, ~4 h at 40−45 °C, ~2 h at 60−65 °C. The drying rate is shown in **Figure 2** to identify the constant and falling rate period. There was no evidence of a constant rate period in drying. The absence of constant rate period indicated that the drying process was internal mass transfer controlled. Analyzing the literature, Rahman and Lamb (*15*) identified that the immediate onset of a falling rate was a characteristic of food materials. The initial drying rates were 3.6, 2.6, and 1.5 kg/h per kilogram of solid for 60−65, 40−45, and 60−65 °C, respectively.

Moisture diffusivity was measured by slope method, and the effective moisture diffusivity was calculated as set forth by Mate et al. (*16*). If the slices are considered as infinite slabs, when MR < 0.6, the effective diffusivity can calculated as (*16*)

$$D_e = \alpha L_0^2/\pi^2 \quad (4)$$

where α is the slope of the ln(MR) (=ln[($X_w - X_{we}$)/($X_{w0} - X_{we}$)]) versus time plot, L_0 is the thickness of a slice (m), D_e is the effective moisture diffusivity (m^2/s), and X_{w0} and X_{we} are the initial and equilibrium moisture contents (wet basis), respectively. The equilibrium moisture content was considered after 24 h of drying. Plots of ln(MR) versus time are shown in **Figure 3**. The slope was estimated for MR < 0.6 as suggested by Mate et al. (*16*). The values of effective diffusivity were estimated as 1.13×10^{-10}, 1.26×10^{-10}, and 2.35×10^{-10} m^2/s, for drying temperatures of 20−25, 40−45, and 60−65 °C, respectively. These are within the values compiled by Sablani et al. (*17*) for apple during drying. As expected, diffusivity increased with the increase of drying temperature.

Changes in Physical Dimension. Table 1 shows the results of the physical changes in apple slices dried at 20−25, 40−45, and 60−65 °C at a relative humidity of 20−25%. These results show that the apple slices dried at 20−25 °C shrank ~14 mm in diameter, whereas those dried at 40−45 °C shrank 10 mm in diameter and those dried at 60−65 °C shrank 8 mm. The results indicated that the higher drying temperatures caused less shrinkage of the slices than the lower (20−25 °C) drying temperature. Similarly, the degree of shrinkage of potato dried at a low drying temperature (40 °C) was found to be greater than that at a high temperature (70 °C) (*18*). It is likely that case hardening occurs in the samples dried at the higher temperature due to the high initial drying rate as shown in **Figure 2**. At a high drying temperature, the external moisture content decreased so quickly that the surface became stiff or rigid (case hardening phenomenon), limiting subsequent shrinkage. This was clearly evident in microscopy studies, which are discussed later.

Table 1. Comparison of the Physical and Microstructure Changes in Dried Apple (Drying Temperature = 20–25, 40–45, 60–65 °C; Relative Humidity = 20–25%)

drying temp (°C)	apple ring diameter (mm) outside fresh	outside dried	core fresh	core dried	dried apple color
20–25	60	46	25	20	light cream
40–45	60	50	25	24	light amber
60–65	60	52	25	26	amber

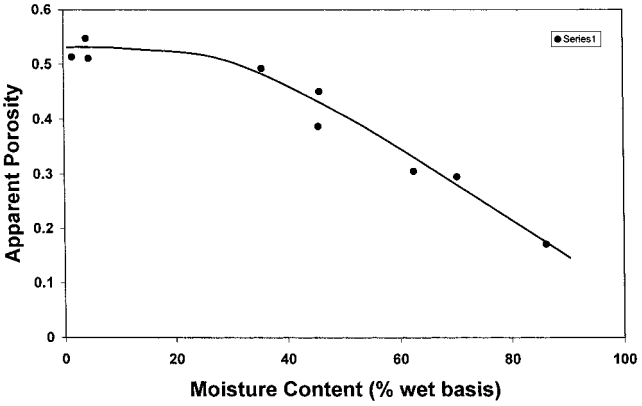

Figure 4. Apparent porosity of dried apple slice as a function of moisture content (drying temperature = 60–65 °C).

Porosity of Dried Apple. Apparent porosity as a function of moisture content is shown in **Figure 4**. Similar results were reported for dried apples (*19*), carrots (*20*), and potato particles (*21*) as a function of water content. Zogzas et al. (1994) studied the drying of apple at 70 ± 0.2 °C in air at a velocity of 2.5 ± 0.1 m/s and relative humidities of 20, 30, 45, and 60%. Their results showed no significant difference in porosity for samples dried at different relative humidities. The apparent porosity of apple slices increased linearly with decrease in water content. When the moisture content was 30%, a constant region was observed.

Shrinkage is the decrease of volume occurring during processing due to the moisture loss during drying and depends on the presence of the formation of pores. Shrinkage is correlated with moisture content as

$$S_a = a[\exp(bX_w)] \quad (5)$$

where a and b are the model parameters, respectively.

Figure 5 shows the experimental and predicted line from the above equation. In most of the literature, the shrinkage was plotted with moisture content to visualize its changes. Data from the literature were compiled, and the coefficients were estimated for different materials (**Table 2**). It was evident that the drying conditions affect the coefficients. The shrinkage as a ratio of (V_a/V_a^0) is needed for engineering design and calculation of the drying process.

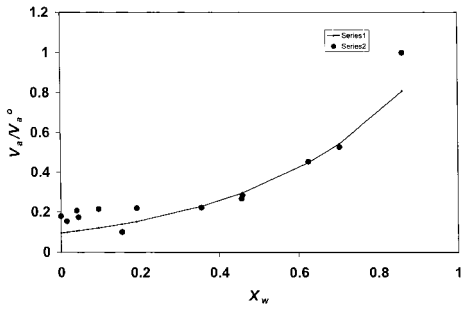

Figure 5. Apparent shrinkage of apple slices dried at 60–65 °C.

Table 2. Values of *a* and *b* for Different Food Materials

material	*T* (°C)[a]	RH (%)[b]	*u*[c] (m/s)	*a*	*b*	ref
apple	60–65	20–25	1.5	0.09	2.50	this work
apple	70	12	3.5	0.29	1.21	Moreira et al. (*26*)
carrot	60	30	1.0	0.06	2.71	Lozano et al. (*20*)
grape	60		2.0	0.14	2.36	Raghavan et al. (*34*)
pear	60	30	1.0	0.08	2.31	Lozano et al. (*26*)
potato	70		4.0	0.17	1.79	Wang and Brennan (*18*)
potato	40		4.0	0.14	2.26	Wang and Brennan (*18*)
potato	40	35	1.0	0.15	1.92	Lozano et al. (*20*)

[a] *T* is drying temperature. [b] RH is relative humidity. [c] *U* is air velocity.

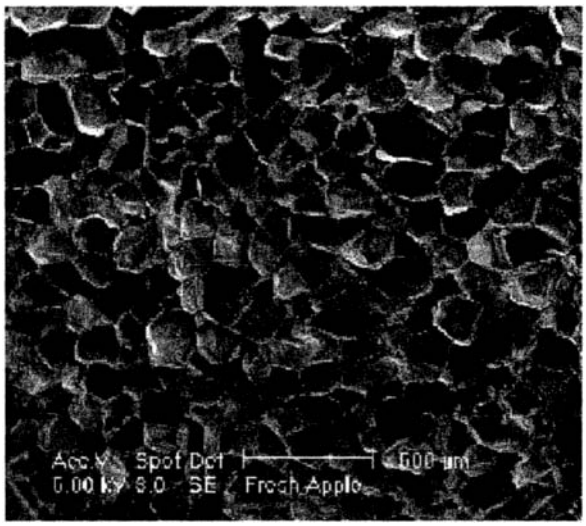

Figure 6. Microstructure of fresh apple.

Microstructure of Dried Apples. Scanning electron micrographs of fresh apple, dried in a critical point drier, are shown in **Figures 6** and **7**. The cell walls are intact and the cells are adhered to one another. There is highly organized cellular compartment of the cells in three-dimensional form in the fresh apple. Some cell damage is apparent and probably occurred during sample preparation. The pores are few and small in size compared to the cells. Similar micrographs of fresh apple were presented by Lee et al. (*23*).

Figure 8 shows the exterior microstructure of apple dried at different temperatures of 20−25 °C (**Figure 8a**), 40−45 °C (**Figure 8b**), and 60−65 °C (**Figure 8c**), at a relative humidity of 20−25%. These micrographs show differences in the exterior microstructure of the apple slices dried at different temperatures. In **Figure 8a** (temperature = 20−25 °C, relative humidity = 20−25%), cells have maintained their three-dimensional organization, but there are some areas where the cells appeared to have collapsed. In addition, there are many pores among the cells. In comparison, **Figure 8b** (temperature = 40−45 °C,

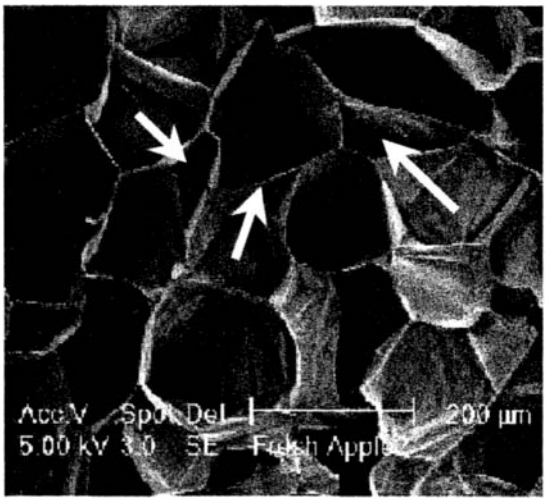

Figure 7. Microstructure of fresh apple at high magnification (arrows indicate the pores).

relative humidity = 20−25%) shows extensive tissue collapse and loss of the three-dimensional form. The surface is quite flattened in appearance and has fewer pores compared with the tissue of the sample dried at 20−25 °C (**Figure 8a**). In **Figure 8c** (temperature = 60−65 °C, relative humidity = 20−25%) the surface of the tissue has collapsed and large cracks have developed. These cracks may be pores that have become connected externally. The results showed that a degree of cellular collapse has occurred in all dried apple slices. Moreover, the higher the drying temperature, the higher the cellular collapse. Comparison of the microstructure of the dried apple samples suggests that case hardening had occurred in the surface of the dried tissue when the apple slices were dried at 40−45 or 60−65 °C. At the highest temperature (60−65 °C) it is possible that additional stress due to extensive casehardening caused cracks to form on the surface (**Figure 8c**). Karathanos et al. (*24*) studied the effective diffusivity and structural changes of starch during air-drying within 60−100 °C. They also indicated that pores and cracks may be formed during the last stage of drying.

Figure 9 shows the microstructure of the interior of the apple slice dried at 20−25 °C (**Figure 9a**), 40−45 °C (**Figure 9b**), and 60−65 °C (**Figure 9c**). As with the exterior view, the interior shows differences in appearance among the apple dried at the different temperatures. All three micrographs show tissue collapse and pore formation. However, the apple dried at 60−65 °C (**Figure 9c**) showed the presence of much larger pores than the other two (**Figure 9ab**), consistent with the exterior view, which showed large cracks. However, the pores in **Figure 9b** were much smaller and fewer in number than those in either panel a or panel c of **Figure 9**. Mavroudis et al. (*25*) compared the osmotic dehydrated apple at 45 and 20 °C and found similar results. They proposed that this is due to the increase in the mechanical strength of the tissue by the activity of the enzyme pectin methyl esterase present in apple. The enzyme has its maximum activity at 45 °C and resulted in enhancement of the cell wall firmness. Therefore, the smaller proportion of pores found at 40−45 °C (**Figure 9b**) may be a consequence of pectin methyl esterase action on cellular integrity. From this study, it was found that the same raw materials may end up as completely different structures depending on the temperature and humidity used in HPD. Depending on the end use of the dried apple, operating conditions could be set up. For example, if we want to use dried apple as an instant soup or noodle ingredient, the dried samples need to have high rehydration capacity. This could

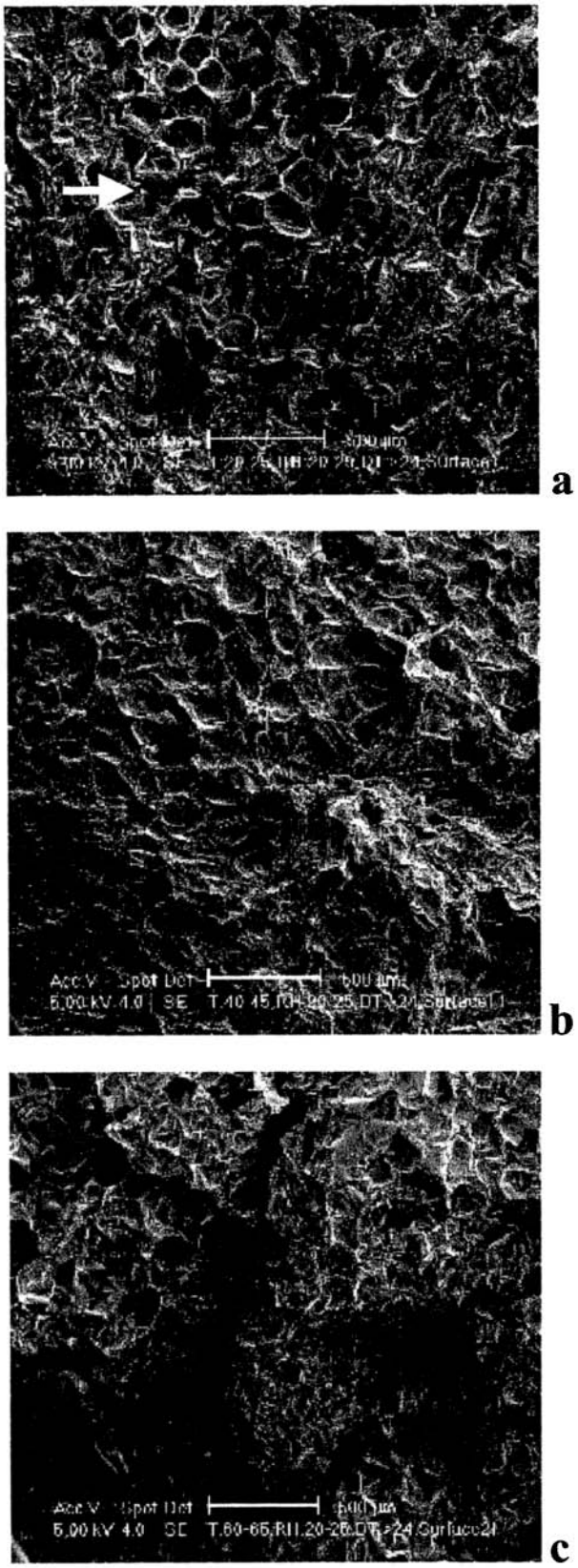

Figure 8. Exterior microstructure of dried apple tissue after drying for 24 h at different temperatures.

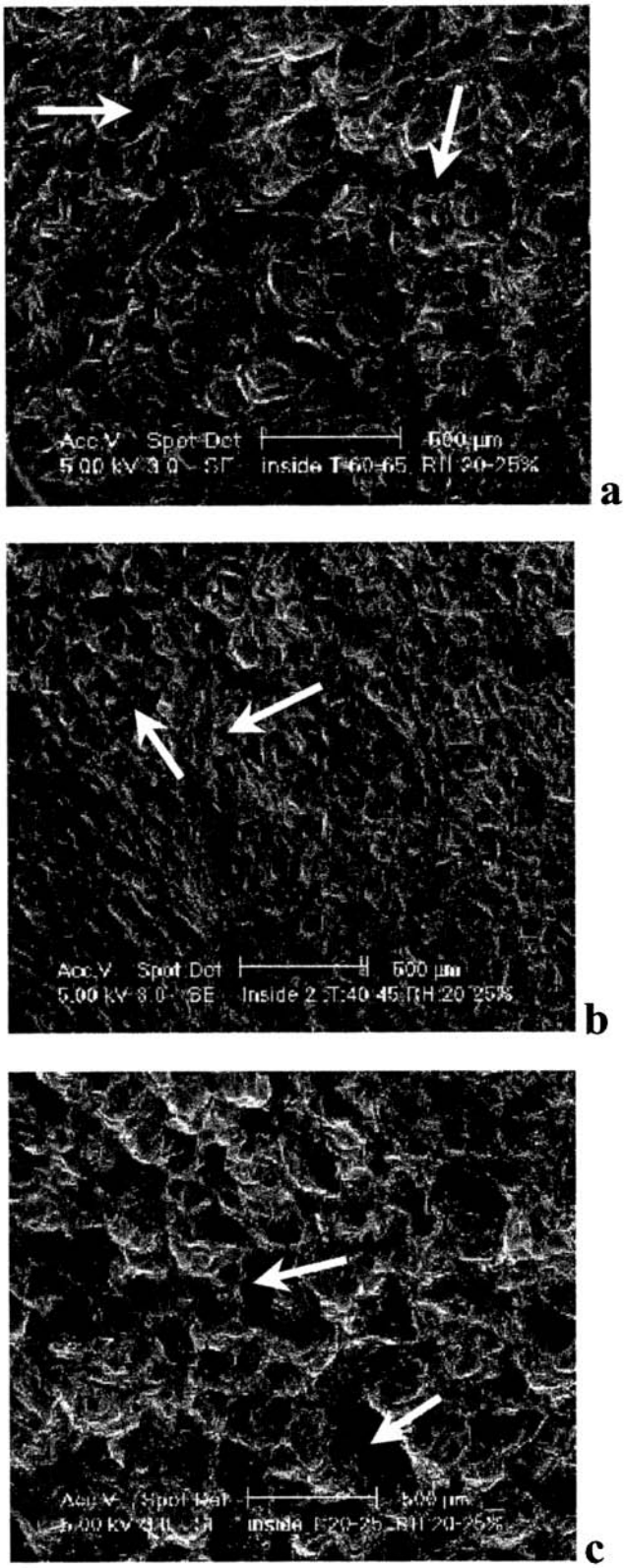

Figure 9. Interior microstructure of the dried apple tissue after drying for 24 h at different temperatures (arrows indicate pores).

be achieved by setting the temperature high and the humidity low in order to form case hardening, which will ultimately form surface cracks. If dried apple is used for breakfast cereals, long bowl life is required. This could be achieved by setting the drying conditions at low temperature to form an impermeable surface with no cracks. Similarly, the nutritional contents could be retained by setting the optimum operating conditions of humidity and temperature. For example, the application of drying air characteristics by elevated relative humidity (15%) and relatively high temperature (90 °C) resulted in better retention of the nutritive value of dried potato (*26*).

No quantitative results are available on the cellular structure damage during drying; thus, only qualitative results from the literature are presented to compare with the above results. Structural damages of the air-dried apples as a function of drying humidity and temperature are not available. For that reason the related results from the literature are discussed below. Wang and Brennan (*18*) studied the structural changes in potato during air-drying (temperatures = 40 and 70 °C) by microscopy. Air humidity values were not presented. They found that shrinkage occurs first at the surface and then gradually moves to the bottom with increase in drying time. The cell walls became elongated. The degree of shrinkage at a low drying temperature (40 °C) was greater than that at high temperature (70 °C). At low drying rate (i.e., at low temperature), the moisture content at the center of a piece is never very much higher than at the surface, internal stresses are minimized, and the material shrinks fully onto a solid core. At higher drying rates the outer layers of the material become rigid and their final volume is fixed early in the drying. As drying proceeds, the tissues split and rupture internally, forming an open structure, and cracks are formed in the inner structure. When the interior finally dries and shrinks, the internal stresses pull the tissue apart. Wang and Brennan did not find any cracks on the surface as was found in the apple in this study. This may be due to the different structural natures of the initial materials. For example, during drying the porosity of dried potato varied from 0.02 to 0.30, whereas the porosity of apple varied from 0.18 to 0.53. Higher porosity (i.e., greater air phase) in the case of apple may create more pressure inside the apple rings; thus, cracks occurred on the surface.

Moreira et al. (*27*) studied the shrinkage of apple rings during convection air-drying (temperature = 70 °C and relative humidity = 12%) and freeze-drying. It was found that shrinkage of samples dried by convection is significantly anisotropic, whereas less damage to the solid structure during freeze-drying leads to a more isotropic deformation. This also suggests that there is a possibility of cracks in the surface due to uneven stress development in the apple sample. Erle and Schubert (*28*) also studied the cell structure of microwave-vacuum-dried apple with and without osmotic treatment. They found collapse of the cellular structure in untreated apple; however, the cell collapse was much lower compared to the heat pump dried samples in this study. They did not study both the surface and interior. Osmotic treatment prior to vacuum-drying preserved the cellular structure by keeping the three-dimensional nature. Vacuum pulse during osmotic dehydration collapsed the cellular structure of the apple as the heat pump dried samples in this study (*29*). Barat et al. (*30*) studied the structure of osmotically treated apple with microscopy. In all cases the structural stresses associated with cell shrinkage promoted osmotic dehydration, and the higher the osmotic concentration, the higher the structural stress. However, this should not be compared with the the results for the air-dried samples. Electron microscopy investigations of the cell structure in dried carrots and green bean showed that drying leads to shrinkage and twisting of the cells and clumping of the cytoplasm (*31*). Lee et al. (*23*) studied the chemical and histological changes in air-dried, freeze-dried, and osmotically treated freeze-dried samples. Air-dried samples showed the elongated and thinned cell wall and enlarged intercellular air spaces. The conditions of drying were not mentioned or identified in their work.

There is negligible information available on the surface structure of dried samples. However, the cracks observed at high temperature could be justified from the related results from the literature. During air-drying, stresses are formed due to nonuniform shrinkage resulting from nonuniform moisture and/or temperature distributions. This may lead to stress crack formation, when stresses exceed a critical level. Crack formation is a complex process influenced interactively by heat and moisture transfer, physical properties, and operational conditions (*32*). Liu et al. (*32*) identified air relative humidity and temperature as the most influential parameters that need to be controlled to eliminate formation of cracks. The increase of drying rate causes the nonuniform distribution of the moisture content in dried material, and this involves the drying-induced stresses (*33*). During drying the final tensile stress level within spaghetti core was responsible for cracking (*34*). Thus, the above discussion explains the reasons for crack formation in samples dried at high temperature with a heat pump.

Conclusion. The structure of food is an important quality parameter for dried food products. The porosity of apple rings increased linearly when the moisture content decreased during drying and then reached a constant value. Differing degrees of cellular collapse were observed by electron microscopy. The degree of surface case hardening was increased with the increase in drying temperature, and at the extreme case cracks were formed on the surface.

LITERATURE CITED

(1) Mason, R. L.; Britnell, P. M.; Young, G. S.; Birchall, S.; Fitz-Payne, S.; Hesse, B. J. Development and application of heat pump dryers to the Australian food industry. *Food Aust.* **1994**, *46*, 319−323.

(2) Perera, C. O.; Rahman, M. S. Heat pump dehumidifier drying of food. *Trends Food Sci. Technol.* **1997**, *8*, 75−79.

(3) Rahman, M. S.; Perera, C. O.; Thebaud, C. Desorption isotherm and heat pump drying kinetics of peas. *Food Res. Int.* **1998**, *30*, 485−491.

(4) Waliuzzaman, Z.; Fletcher, G.; Rahman, M. S.; Perera, C. O. The microflora changes in fish mince during heat pump dehumidifier drying. In *10th World Congress of Food Science and Technology*, Sydney, Oct 3−8, 1999.

(5) Prichavudhi, K.; Yamamoto, H. Y. Effect of drying temperature on chemical composition and quality of macadamia nuts. *Food Technol.* **1965**, *19*, 1153.

(6) Van Blarcom, A.; Mason, R. L. Low humidity drying of macadamia nuts. In *Proceedings of the Fourth Australian Conference on Tree and Nut Crops*, Lismore, NSW, 1988; p 239.

(7) Minemoto, Y.; Adachi, S.; Matsuno, R. Comparison of oxidation of methyl linoleate encapsulated with gum arabic by hot-air-drying and freeze-drying. *J. Agric. Food Chem.* **1997**, *45*, 4530−4534.

(8) Prestamo, G.; Fuster, C.; Risueno, M. C. Effect of blanching and freezing on the structure of carrots cells and their implications for food. *J. Sci. Food Agric.* **1998**, *77*, 223−229.

(9) Hershko, V.; Nussinovitch, A. Relationships between hydrocolloid coating and mushroom structure. *J. Agric. Food Chem.* **1998**, *46*, 2988−2997.

(10) Rahman, M. S.; Al-Amri, O. S.; Al-Bulushi, I. M. Pores and physico-chemical characteristics of dried tuna produced by different methods of drying. *J. Food Eng.* **2002** (in press).

(11) Rahman, M. S. In *Food Properties Handbook*; CRC Press: Boca Raton, FL, 1995; pp 87−122.

(12) Gejl-Hansen, F.; Flink, J. M. Application of microscopic techniques to the description of structure of dehydrated food systems. *J. Food Sci.* **1976**, *41*, 483−489.

(13) Flink, J. M.; Gejl-Hansen, F.; Karel, M. Microscopic investigations of the freeze-drying of volatile-containing model food solutions. *J. Food Sci.* **1973**, *38*, 1174−1178.

(14) Gejl-Hansen, F.; Flink, J. M. Freeze-dried carbohydrate containing oil-in-water emulsions: microstructure and fat distribution. *J. Food Sci.* **1977**, *42*, 1049−1055.
(15) Rahman, M. S.; Lamb, J. Air drying behavior of fresh and osmotically dehydrated pineapple. *J. Food Process Eng.* **1991**, *14*, 163−171.
(16) Mate, J. I.; Quartaert, C.; Meerdink, G.; Riet, K. V. Effect of blanching on structural quality of dried potato slices. *J. Agric. Food Chem.* **1998**, *46*, 676−681.
(17) Sablani, S.; Rahman, M. S.; Al-Habsi, N. Moisture diffusivity in foods—an overview. In *Drying Technology in Agricultural and Food Sciences*; Mujumdar, A. S., Ed.; Science Publishers: Enfield, NH, 2000; pp 35−59.
(18) Wang, N.; Brennan, J. G. Changes in structure, density and porosity of potato during dehydration. *J. Food Eng.* **1995**, *24*, 61−76.
(19) Lozano, J. E.; Rostein, E.; Urbicain, M. J. Total porosity and open-pore porosity in the drying of fruits. *J. Food Sci.* **1980**, *45*, 1403−1407.
(20) Lozano, J. E.; Rostein, E.; Urbicain, M. J. Shrinkage, porosity and bulk density of foodstuffs at changing moisture contents. *J. Food Sci.* **1983**, *48*, 1497−1501.
(21) Ratti, C. Shrinkage during drying of foodstuffs. *J. Food Eng*. **1994**, *23*, 91−105.
(22) Zogzas, N. P.; Maroulis, Z. B.; Marinos-Kouris, D.; Saravacos, G. D. Densities, shrinkage and porosity of some vegetables during air-drying. In *Drying '94, Proceedings of the 9th International Drying Symposium (IDS'94)*, Gold Coast, Australia, Aug 1−4, 1994; pp 863−870.
(23) Lee, C. Y.; Salunkhe, D. K.; Nury, F. S. Some chemical and histological changes in dehydrated apple. *J. Sci. Food Agric.* **1967**, *18*, 89−93.
(24) Karathanos, V. T.; Villalobos, G.; Saravacos, G. D. Comparison of two methods of estimating of the effective moisture diffusivity from drying data. *J. Food Sci.* **1990**, *55*, 218−231.
(25) Mavroudis, N. E.; Wadso, L.; Gekas, V.; Sjoholm, I. Shrinkage, microscopic studies and kinetics of apple fruit tissue during osmotic dehydration. In *Presented at 11th International Drying Symposium (IDS'98)*, Halkidiki, Greece, Aug 19−22, 1998; pp 844−851.
(26) Iciek, J.; Krysiak, W. The conditions of convention drying of potatoes and their effect on the nutritive value of the product. In *Properties of Water in Foods*; Lewicki, P. P., Ed.; Warsaw Agricultural Press: Warsaw, Poland, 1996; pp 35−20.
(27) Moreira, R.; Villate, J. E.; Figueiredo, A.; Sereno, A. Shrinkage of apple slices during drying by warm air convection and freeze-drying. In *Drying '98—Proceedings of the 11th International Drying Symposium*, Halkidiki, Greece, 1998; pp 1108−1114.
(28) Erle, U.; Schubert, H. Combined osmotic and microwave-vacuum dehydration of apples and strawberries. *J. Food Eng.* **2001**, *49*, 193−199.
(29) Barat, J. M.; Fito, P.; Chiralt, A. Modeling of simultaneous mass transfer and structural changes in fruit tissues. *J. Food Eng.* **2001**, *49*, 77−85.
(30) Barat, J. M.; Albors, A.; Chiralt, A.; Foto, P. Equilibration of apple tissue in osmotic dehydration microstructural changes. In *Drying '98—Proceedings of the 11th International Drying Symposium*, Halkidiki, Greece, 1998; pp 827−835.
(31) Grote, M.; Fromme, H. G. Electron microscopic investigations of the cell structure in fresh and processed vegetables (carrots and green bean pods). *Food Microstruct.* **1984**, *3*, 55−64.
(32) Liu, H.; Zhou, L.; Hayakawa, K. Sensitivity analysis for hygrostress crack formation in cylindrical food during drying. *J. Food Sci.* **1997**, *62*, 447−450.
(33) Kowalski, S. J.; Rybicki, A. Drying induced stresses and their control. In *Drying '96—Proceedings of the 10th International Drying Symposium*, Krakow, Poland, 1996; pp 151−158.
(34) Peczalski, R.; Laurent, P.; Andrieu, J.; Boyer, J. C.; Boivin, M. Drying-induced stress build-up within spaghetti. In *Drying '96—Proceedings of the 10th International Drying Symposium*, Krakow, Poland, 1996; pp 805−816.
(35) Raghavan, G. S. V.; Tulasidas, T. N.; Sablani, S. S.; Ramaswamy, H. S. Concentration dependent moisture diffusivity in drying of shrinkable commodities. In *Proceedings of the 9th International Drying Symposium*, Gold Coast, Australia; 1994; pp 1−4.

Received for review October 11, 2001. Revised manuscript received February 5, 2002. Accepted March 6, 2002.

JF011354S